Journal of
Ceramic Science
and Technology

J. Ceram. Sci. Tech., **05** [02] 93-100 (2014)
DOI: 10.4416/JCST2013-00024
available online at: http://www.ceramic-science.com

Synthesis of $LaCrO_3$ and $La_{0.9}Ca_{0.1}CrO_3$ by Modified Glycine Nitrate Process

A. Bonet*, N. Travitzky*, P. Greil

University of Erlangen-Nuremberg, Department of Materials Science (Glass and Ceramics), Martensstr. 5, D-91058 Erlangen, Germany

received October 11, 2013; received in revised form December 1, 2013; accepted March 11, 2014

Abstract

$LaCrO_3$ and $La_{0.9}Ca_{0.1}CrO_3$ ceramics were synthesized in the modified glycine nitrate process (MGNP). The effect of the equivalence ratio Φ_e of precursor mixtures on the combustion reaction was investigated by means of DSC and TG-FTIR analyses. It was found that for $\Phi_e > 0.65$ the combustion reaction proceeds in a self-propagating one-step process, resulting in the formation of well-crystallized single-phase powders. Further glycine addition ($\Phi_e < 0.65$) leads to sluggish multi-step combustion, which is typical for fuel-rich combustion, and the formation of secondary phases such as La_2CrO_6. Furthermore it could be found that the ignition temperature of the precursors rises with rising fuel content. An influence of the equivalence ratio on the specific surface area and particle size of synthesized powders could not be detected. The specific surface area of the powders was in the range of 5 – 10 m^2/g and particle size 100 – 150 nm.

Keywords: Lanthanum chromite, modified glycine nitrate process, combustion synthesis

I. Introduction

Lanthanum chromite, $LaCrO_3$, is a refractory oxide with distorted perovskite structure [1]. Owing to their high electrical conductivity and high-temperature stability in oxidizing and reducing atmospheres, lanthanum-chromite-based ceramics have been investigated extensively as interconnectors in solid oxide fuel cells (SOFC) [2,3,4], as heating elements at high temperatures > 1450 °C in oxidizing atmosphere [5,6,7] and as hot electrodes for MHD power generation [8]. In an oxidizing atmosphere, vaporization of the chromium species gives rise to poor sinterability [9]. The main strategies to improve the sinterability of $LaCrO_3$ are (1) sintering in a reducing atmosphere [10], (2) use of nanoscale powders with high sintering activity [11], (3) Cr-deficient stoichiometry [12,13], (4) doping with earth alkali metals [11,14] and (5) use of sintering aids such as strontium vanadate [15].

Nanoscale powders with a high specific surface area and high packing density may enhance the sintering activity of ceramics. Nanoscale perovskite powders can be synthesized in the glycine nitrate process (GNP) [16]. In this process, metal nitrates and glycine are dissolved in water. Glycine complexes the metal ions with its carboxylic acid and amine group (zwitterionic glycine), to prevent selective precipitation during water evaporation. Furthermore, glycine serves as fuel that is oxidized by the nitrate groups. Heating up the aqueous solution leads at first to evaporation of water and at approximately 180 °C to spontaneous combustion of the viscous liquid, resulting in the formation of an ash containing the perovskite reaction product. Depending on glycine/nitrate ratio, this high exothermic redox reaction reaches flame temperatures up to 1450 °C and is completed in a few seconds. The peak flame temperature (maximum energy release) is reached at a stoichiometric glycine/nitrate ratio of 0.56, forming only H_2O, CO_2 and N_2 with no atmospheric oxygen being required [16]. An example of this combustion reaction for synthesis of perovskite oxides ($A^{3+}B^{3+}O_3$) can be described as follows:

$$3A(NO_3)_3 + 3B(NO_3)_3 + 10C_2H_5NO_2 \rightarrow ABO_3 + 25H_2O + 20CO_2 + 14N_2 \quad (1)$$

Compared to the mixed oxide route, GNP is a fast and simple method to produce nanoscale (5 – 50 nm particle size) single- [17,18,19] and multi-oxide powders [20,21,22,23] with a high specific surface area and homogeneous composition [16]. Owing to its high exothermic nature and high amount of released gases, however, this reaction is difficult to control. Bošković *et al.* modified the glycine nitrate process with partial substitution of nitrates by acetates (MGNP) [20] in order to reduce the reaction rate and to facilitate reaction control. For the glycine nitrate process a lot of work has been done to investigate the influence of the glycine/nitrate ratio on the combustion reaction and the resulting powder [23,24,25]. However, owing to substitution of nitrates by acetates, this work is not transferable to the MGNP. In order to control the synthesis reaction, it is essential to understand the effect of partial substitution of nitrates by acetates. Thus, it is the aim of this work to investigate the effect of the fuel/oxidant ratio on the combustion reaction and synthesized $LaCrO_3$-based perovskite in the modified glycine nitrate process.

* Corresponding author: Alexander.Bonet@fau.de, nahum.travitzky@ww.uni-erlangen.de

Table 1: Composition and equivalence ratio of used precursors.

Sample	*Composition*	Φ_e
LC-11-0	$La(CH_3COO)_3$ + $Cr(NO_3)_3$	0.7692
LC-11-1	$La(CH_3COO)_3$ + $Cr(NO_3)_3$ + 1 $C_2H_5NO_2$	0.6538
LC-11-2	$La(CH_3COO)_3$ + $Cr(NO_3)_3$ + 2 $C_2H_5NO_2$	0.5846
LC-11-3	$La(CH_3COO)_3$ + $Cr(NO_3)_3$ + 3 $C_2H_5NO_2$	0.5385
LC-11-4	$La(CH_3COO)_3$ + $Cr(NO_3)_3$ + 4 $C_2H_5NO_2$	0.5055
LC-11-5	$La(CH_3COO)_3$ + $Cr(NO_3)_3$ + 5 $C_2H_5NO_2$	0.4808
LCC-911-0	0.9 $La(CH_3COO)_3$ + 0.1 $Ca(NO_3)_3$ + $Cr(NO_3)_3$	0.8427
LCC-911-1	0.9 $La(CH_3COO)_3$ + 0.1 $Ca(NO_3)_3$ + $Cr(NO_3)_3$ + 1 $C_2H_5NO_2$	0.6996
LCC-911-2	0.9 $La(CH_3COO)_3$ + 0.1 $Ca(NO_3)_3$ + $Cr(NO_3)_3$ + 2 $C_2H_5NO_2$	0.6169
LCC-911-3	0.9 $La(CH_3COO)_3$ + 0.1 $Ca(NO_3)_3$ + $Cr(NO_3)_3$ + 3 $C_2H_5NO_2$	0.5630
LCC-911-4	0.9 $La(CH_3COO)_3$ + 0.1 $Ca(NO_3)_3$ + $Cr(NO_3)_3$ + 4 $C_2H_5NO_2$	0.5251
LCC-911-5	0.9 $La(CH_3COO)_3$ + 0.1 $Ca(NO_3)_3$ + $Cr(NO_3)_3$ + 5 $C_2H_5NO_2$	0.4970

II. Experimental Procedure

(1) Powder synthesis

Starting chemicals for $LaCrO_3$ and $La_{0.9}Ca_{0.1}CrO_3$ synthesis were glycine (Merck), lanthanum acetate sesquihydrate (Alfa Aesar, 99.9 %), calcium nitrate tetrahydrate (Merck, ACS) and chromium nitrate nonahydrate (Sigma Aldrich, 99 %). All starting chemicals were dissolved in water and the concentration of metal ions of aqueous solutions was controlled by means of ICP spectroscopy (Spectro, Genesis SOP). Stoichiometric amounts of metal ion solutions were mixed and placed in a high heat-resistant steel reactor. The aqueous precursor solution was heated up to 800 °C at a heating rate of 10 K/min and held for a half hour. Owing to partial substitution of nitrates by acetates, the glycine/nitrate ratio of the precursor is no longer meaningful. Therefore, it is more practical to evaluate the precursor mixtures based on an equivalence ratio Φ_e [26],

$$\Phi_e = \frac{\sum x_i^{ox} \cdot n^-}{(-1) \cdot \sum x_i^{red} \cdot m^+} \qquad (2)$$

where x_i^{ox} and x_i^{red} denote the coefficient of oxidizing and reducing elements and n^- and m^+ the corresponding valences. La, Ca, Cr, C and H were set as reducing elements and O as oxidizing element. N was always considered as neutral, assuming that nitrogen reacts only to N_2. The valence of the oxidizing elements was considered as negative and valence of the reducing elements as positive. An equivalence ratio $\Phi_e = 1$ represents a stoichiometric mixture, $\Phi_e > 1$ fuel-lean and $\Phi_e < 1$ fuel-rich conditions, respectively. The composition of precursor mixtures and their equivalence ratio Φ_e are summarized in Table 1.

In order to study the exothermicity of the synthesis process, depending on glycine content, the enthalpy change of combustion reaction was calculated with Equation (3),

$$\Delta H^0 = \sum n \cdot \Delta H^0_{f\,products} - \sum n \cdot \Delta H^0_{f\,reactants} \qquad (3)$$

with n as the number of moles and ΔH_f^0 as the standard enthalpy of the formation of reactants and products respectively. For simplification, oxygen excess from air was considered as high enough for complete combustion to produce only H_2O, CO_2 and N_2 for all precursors. Adiabatic combustion temperature of reactions was calculated according to Equation (4),

$$\Delta H^0 + \int_{T_0}^{T_{ad}} \sum (n \cdot c_p)_{products} dT = 0 \qquad (4)$$

where ΔH^0 is the enthalpy change of reaction, $T_0 = 298.15$ K (25 °C), c_p the heat capacity and n the moles of corresponding reaction product. The adiabatic flame temperature is the theoretically maximum temperature that can be achieved for given reactants, considering that reaction proceeds under adiabatic conditions and no energy is lost. Under these assumptions, the complete ΔH^0 is consumed by the specific heat capacity of reaction products, whereby these are heated up to T_{ad}. All necessary thermodynamic data for calculation of ΔH^0 and T_{ad} are summarized in Table 2.

(2) DSC and TGA-FTIR analyses

Small amounts of aqueous precursor solutions were dried in a drying chamber at 110 °C. The resulting gels were used for DSC (Du Pont Instruments, 910 DSC) and TGA-FTIR (Netzsch, TG 209 F1; Bruker, Tensor 27) analyses. TG-FTIR analyses were conducted only on LCC-911 precursors, because no difference in the degradation products to LC-11 is expected. Measurements were conducted up to 600 °C (DSC) and 900 °C (TGA-IR) with a heating rate of 10 K/min in air atmosphere. For comparison, TGA-FTIR was also conducted on all pure chemicals in the same conditions.

Table 2: Thermodynamic data of reactants and reaction products.

Products	*Reactants*	ΔH_f^0 [kJ/mol]	c_p [J/mol·K]
$LaCrO_3$ (s)		-1534.4	$119.300+12.050\cdot10^{-3}\cdot T-14.640\cdot10^{5}\cdot T^{-2}$
H_2O (g)		-241.8	$31.437+14.105\cdot10^{-3}\cdot T-24.952\cdot10^{5}\cdot T^{-2}-1.832\cdot10^{-6}\cdot T^{2}$
CO_2 (g)		-393.5	$54.435+5.116\cdot10^{-3}\cdot T-43.578\cdot10^{5}\cdot T^{-2}-0.806\cdot10^{-6}\cdot T^{2}$
N_2 (g)		0.0	$23.529+12.116\cdot10^{-3}\cdot T+1.210\cdot10^{5}\cdot T^{-2}-3.076\cdot10^{-6}\cdot T^{2}$
	$La(CH_3COO)_3$ (s)	-2208.8	
	$Cr(NO_3)_3$ (s)	-858.2	
	$C_2H_5NO_2$ (s)	-528.1	

(3) Powder characterization

The phase composition of the synthesized powders was characterized by means of X-ray powder diffraction (Siemens, Kristalloflex D500) in an angle range of 5 – 70°. Cu-Kα radiation with a wavelength of 0.154 nm was used. The density was measured with a He-pycnometer (Micromeritics, AccuPyc 1340) and the specific surface area with the nitrogen adsorption method (Micromeritics, ASAP 2000). The particle size was calculated from density and specific surface area data, assuming that particles are ideally spherical.

III. Results and Discussion

(1) Combustion of precursors

TGA-IR and DSC were used to determine the decomposition of the precursor mixtures used in order to comprehend the combustion process. In Fig. 1, the ignition temperature of precursors is shown as a function of Φ_e. Thereby, the ignition temperature was defined by the temperature of the first exothermic peak value in the DSC curve, related to combustion of organic compounds. It can be seen that the rising approach to stoichiometric precursor composition ($\Phi_e = 1$) reduces the ignition temperature, with the exception of LC-11-0 and LCC-911-0. The essential reduction of the ignition temperature with rising Φ_e may be explained by higher reactivity, owing to the higher oxygen content in the precursor for necessary combustion [27]. Although precursors LC-11-0 and LCC-911-0 have the highest Φ_e, their ignition temperatures are the highest too. This could be explained by selective precipitation of raw materials owing to the missing glycine. Glycine-metal complexes enhance the uniform mixture of reactants in the precursor at the atomic or molecular level. Thus, the nucleation process can occur as a result of the rearrangement and short diffusion path of nearby atoms and molecules during the combustion process [28], resulting in a reduced ignition temperature in contrast to precipitated reactants.

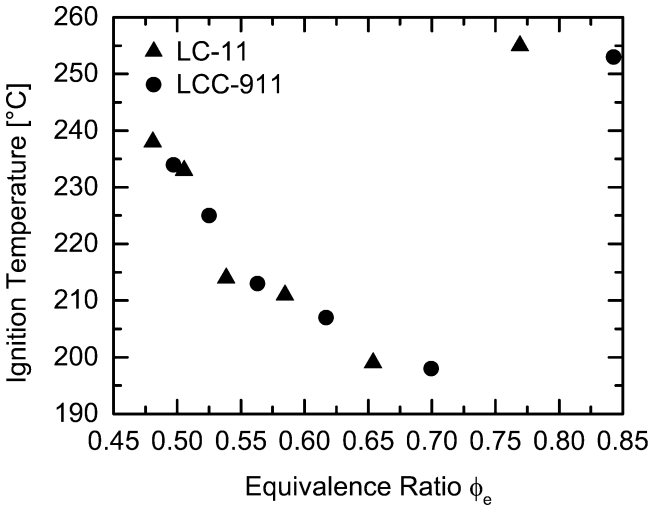

Fig. 1: Ignition temperature as function of equivalence ratio.

TG/DTG and DSC curves of precursors LCC-911-0, -1 and -3 are shown in Fig. 2. The curves of other precursors are not presented because they do not differ significantly from that of LCC-911-3. A clear difference in the combustion process of these three precursors can be seen. Combustion of the glycine-free precursor LCC-911-0 (A) takes place in several steps. Up to temperatures of 273 °C, water is evaporated. At approximately 244 °C, combustion of the organic compounds starts. In aqueous solution acetate groups form acetic acid, which evaporates and decomposes with rising temperature according to Reaction (5). At approximately 300 °C, further oxidation of the acetic acid takes place according to Reaction (6),

$$C_2H_4O_2 + 2O_2 \rightarrow 2CO_2 + H_2O \tag{5}$$

$$k\,C_2H_4O_2 \rightarrow k\,CH_4 + l\,CO_2 + (k\text{-}l)CO + \left(\frac{k-l}{2}\right)O_2 \tag{6}$$

with k and l as the coefficient of the glycine and formed carbon dioxide on condition that $l \leq k$. With a further increase in temperature, only Reaction (5) occurs. Nitrate ions, which act as an oxidizer, decompose according to Reaction (7),

$$m\,NO_3^- \rightarrow n\,N_2 + o\,NO_2 + pNO + \left(\frac{3m-2o-p}{2}\right)O_2 \tag{7}$$

with m as the coefficient of the nitrate ions and n, o and p as the coefficient of the formed N_2, NO_2 and NO, respectively, provided that 2n + o + p = m. Up to temperatures of 400 °C, NO_2 and NO could be detected. Higher temperatures seem to enhance the formation of NO_2.

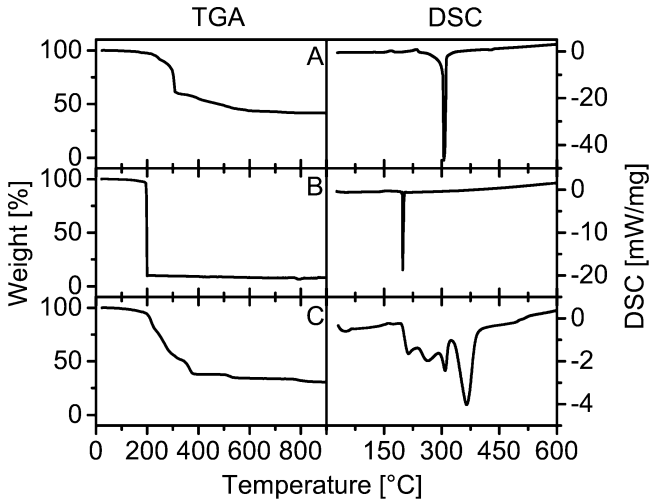

Fig. 2: TGA and DSC curves of precursor LCC-911-0 (A), LCC-911-1 (B) and LCC-911-3 (C).

Precursor LCC-911-1 (B) decomposes at about 200 °C in a self-propagating one-step process. Thereby, acetate ions decompose according to Reactions (5) and (6). The decomposition of the nitrate ions follows Reaction (7) with the limitation that o = 0. Release of N_2 and O_2 is probable, but cannot be detected by FTIR-spectroscopy in air atmosphere. Possible combustion reactions of glycine are presented by (8) and (9), with r, s and u as the coefficient of the glycine and formed CO_2 and NO respectively, on condition that $2s \leq r \cap u \leq r$.

$$r\,C_2H_5NO_2 + \frac{s+r}{2}\,O_2 \rightarrow r\,NH_3 + s\,CO_2 + (2r-s)\,CO + r\,H_2O \quad (8)$$

$$r\,C_2H_5NO_2 + \frac{s+2.5r+u}{2}\,O_2 \rightarrow s\,CO_2 + (2r-s)\,CO + 2.5r\,H_2O + u\,NO + \left(\frac{r-u}{2}\right)N_2 \quad (9)$$

Precursor LCC-911-3 (C) decomposes at about 216 °C in a sluggish multi-step process. Acetate ions decompose according to Reaction (5) and nitrate ions according to Reaction (7). Oxidation of glycine takes place according to Reactions (8) and (9), similar to precursor LCC-911-1. For the weight loss at approximately 790 °C no gaseous species could be detected. This decomposition step could be assigned to oxygen release of the formed intermediate phase $LaCrO_4$, which is known to proceed in the temperature range of about 700 °C [14], according to Reaction (10).

$$LaCrO_4 \rightarrow LaCrO_3 \rightarrow 0.5\,O_2 \quad (10)$$

Similar combustion behavior of fuel-rich glycine-nitrate precursors for $La_{0.7}Ca_{0.3}CrO_3$ synthesis was described by Nair *et al.* [27]. They found a single-step decomposition behavior of stoichiometric and slightly fuel-rich precursors and sluggish multi-step combustion for further fuel addition. The ignition temperature was also higher for the precursor with higher fuel content. This suggests that modification of the glycine nitrate process by partial substitution of metal nitrate by metal acetate [20], in order to facilitate reaction control, reduces the reaction rate of the combustion reaction owing to the fuel richness of the precursor, comparable to fuel-rich glycine-nitrate precursors.

Calculated ΔH^0 and T_{ad} of the precursors used are presented in Table 3. It has to be considered that T_{ad} is only a theoretical value and the temperatures reached during combustion processes are much lower [16]. But none the less T_{ad} is used to describe the theoretical potential of a combustion system and to evaluate the effect of variation of fuel/oxidizer mixtures on the combustion process. Owing to the higher fuel content of glycine-rich precursors and the assumption of enough oxygen access from the atmosphere for complete combustion, ΔH^0 and T_{ad} rise with rising glycine content. It has to be considered that the used heat capacities of products for calculation are defined for the temperature range of about 900-2800 K. Thus, they are inaccurate for the wide temperature range from 298 K up to the calculated T_{ad}, which leads to a defective calculated T_{ad}. But the trend is meaningful. Calculation of T_{ad} without oxygen excess from the atmosphere was not possible for precursors LC-11-2, -3, -4 and -5, owing to the high fuel richness of these precursors. This high fuel richness leads to the formation of only H_2 and CO instead of H_2O and CO_2, which results in endothermic ΔH^0.

Table 3: Enthalpy of reaction and adiabatic flame temperature of precursors with and without oxygen access from atmosphere.

		With oxygen access from atmosphere		*Without oxygen access from atmosphere*	
Sample	Φ_e	ΔH^0 [kJ/mol]	T_{ad} [K]	ΔH^0 [kJ/mol]	T_{ad} [K]
LC-11-0	0.7692	-1899.572	2926	-627.029	1393
LC-11-1	0.6538	-2763.215	3133	-259.336	636
LC-11-2	0.5846	-3626.858	3264	46.544	-
LC-11-3	0.5385	-4490.502	3338	352.424	-
LC-11-4	0.5055	-5354.145	3396	658.305	-
LC-11-5	0.4808	-6217.788	3439	964.185	-

(2) Powder characterization

The phase composition of synthesized powders is shown in Fig. 3. As a result of the heating up to 800 °C, all powders were well crystallized after synthesis. The main phase of the powders is $LaCrO_3$ and $La_{0.9}Ca_{0.1}O_3$ for the LC-11 and LCC-911 precursors, respectively. The precursors without glycine showed a significant amount of secondary phases such as La_2CrO_6, $LaCrO_4$ and $CaCrO_4$. $LaCrO_4$ is an intermediate phase during $LaCrO_3$ formation, which decomposes according to Reaction (10) to $LaCrO_3$ at temperatures > 700 °C [14]. The

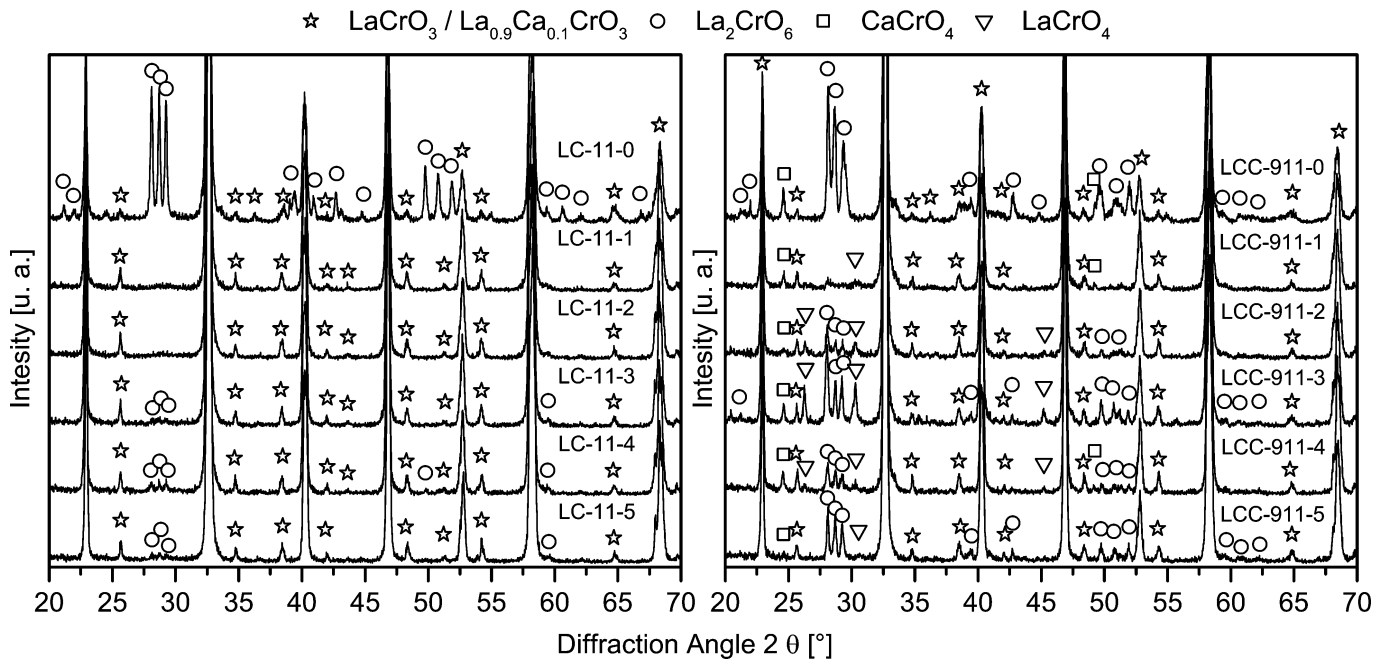

Fig. 3 : Phase composition of synthesized powders.

$LaCrO_4$ content in the powder denotes that the combustion temperature and/or holding time at 800 °C was not high enough for complete reduction of $LaCrO_4$ to $LaCrO_3$. $CaCrO_4$ formation is due to the limited solubility of Ca in $LaCrO_3$ lattice at low temperatures [29]. Ianculescu *et al.* [30] described La_2CrO_6 formation during synthesis of $LaCrO_3$ by solid state reaction owing to the trend of chromium to oxidize from Cr^{3+} to Cr^{6+} at temperatures < 1000 °C. At higher temperatures, La_2CrO_6 decomposes to $LaCrO_3$. Zupan *et al.* [31] also explained La_2CrO_6 formation during combustion synthesis of $LaCrO_3$ owing to low temperatures during synthesis. Glycine-containing precursors showed a rising trend to La_2CrO_6 formation with rising glycine content. This trend is higher for $La_{0.9}Ca_{0.1}CrO_3$ than for $LaCrO_3$. Although reaction enthalpy and adiabatic flame temperatures rise with increasing glycine content, the temperature during synthesis seems to decrease. A possible explanation could be found in a different reaction mechanism. As shown in Fig. 2, the glycine-containing precursor LC-11-1 combusts in a self-propagating one-step combustion process. So the whole reaction enthalpy is released at one point, resulting in the generation of a high temperature which could suppress secondary phase formation and/or decompose secondary phases such as La_2CrO_6. Increasing glycine content leads to a sluggish multi-step combustion process which is typical for fuel-rich combustion [32], where the reaction enthalpy is released in several steps. So the maximum temperature that can be achieved is decreased. An additional calcination process at temperatures > 1000 °C could be used for decomposition of La_2CrO_6, but would also lead to particle growth and thereby cancel the advantage of the small particle size of combustion synthesis. So it is more practical to avoid La_2CrO_6 formation during synthesis.

Table 4: Density, specific surface area and calculated particle size of synthesized powders.

Sample	*Density*	*Specific Surface Area*	*Average Particle Size*
	[g/cm³]	*[m²/g]*	*[nm]*
LC-11-0	6.69	6.0	150
LC-11-1	6.98	7.3	119
LC-11-2	6.83	6.5	135
LC-11-3	6.68	9.5	94
LC-11-4	6.70	6.6	135
LC-11-5	6.78	7.1	124
LCC-911-0	5.78	5.7	181
LCC-911-1	6.35	5.8	164
LCC-911-2	6.38	6.2	153
LCC-911-3	6.16	6.3	154
LCC-911-4	6.26	5.7	168
LCC-911-5	6.33	7.3	130

The measured specific surface area, density and calculated average particle size are shown in Table 4. It has to be taken into account that the average particle size was calculated on the basis of certain assumptions. The biggest effect on possible error in the calculation is the particle shape. In this work it was supposed that particles are ideally spherical. As seen from other works, powders synthesized by GNP are near to this spherical shape, but an exact deviation is not known [33]. Furthermore it has to be considered that measurement of the specific surface area with the BET method is defective [34], owing to the required simplification for the calculation of the surface area by this method.

So the absolute values of the specific surface area and average particle size are not meaningful, but they are suited for comparison between the synthesized samples. There is no recognizable trend, neither within a series nor between the series. For the measured density it has to be considered that most samples contain small amounts of secondary phases. So, the measured density is an averaged density depending on amount and type of secondary phases. Generally, the measured specific surface area is lower and thus the particle size larger than reported elsewhere [31] for combustion-synthesized lanthanum-chromite-based perovskites. A reason could be the experimental procedure applied. In contrast to other works, the precursor gel was not heated on a hot plate up to the point of auto ignition, but heated in a furnace up to 800 °C and held for a half hour. This could be seen as a combination of synthesis and calcination. This exposure to high temperature may lead to particle growth of the synthesized powder.

IV. Conclusions

The influence of the fuel-oxidizer ratio on combustion synthesis of lanthanum-chromite-based ceramics in the modified glycine nitrate process was investigated. Depending on the equivalence ratio Φ_e of the precursor mixture, different combustion mechanisms were found. For precursors containing 1 mol glycine ($\Phi_e = 0.65 - 0.70$), a self-propagating one-step combustion process was indicated, which leads to well-crystallized single-phase $LaCrO_3/La_{0.9}Ca_{0.1}CrO_3$ powder. Further addition of glycine leads to a sluggish multi-step combustion process, which is typical for fuel-rich combustion, resulting in the formation of secondary phases such as $LaCrO_4$ and La_2CrO_6. Compared to the standard glycine nitrate process, modification by partial substitution of nitrates with acetates enhances the fuel richness of the precursor mixture and leads thereby to a sluggish multi-step combustion reaction that can be better controlled.

Acknowledgement

The authors thank the DFG for its support in the scope of the project SPP1418 FIRE GR961/31.

References

[1] Hashimoto, T., Takagi, K., Tsuda, K., Tanaka, M., Yoshida, K., Tagawa, H., Dokiya, M.: Determination of the space group of $LaCrO_3$ by convergent-beam electron diffraction, *J. Electrochem. Soc.*, **147**, 4408 – 4410, (2000).

[2] Minh, N.Q.: Ceramic fuel cells, *J. Am. Ceram. Soc.*, **76**, 563 – 588, (1993).

[3] Fergus, J.W.: Lanthanum chromite-based materials for solid oxide fuel cell interconnects, *Solid State Ionics*, **171**, 1 – 15, (2004).

[4] Zhu, W.Z., Deevi, S.C.: Development of interconnect materials for solid oxide fuel cells, *Mater. Sci. Eng.*, **A348**, 227 – 243, (2003).

[5] Wakisaka, K., Kado, H., Yoshikado, S.: Fabrication and evaluation of ca, Sr-doped-$LaCrO_3$ thin film electric heaters, *Key Eng. Mat.*, **269**, 121 – 124, (2004).

[6] Suvorov, S., Zuev, A., Pozniak, I., Pechenkov, A., Shatunov, A., Kydryash, M., Niemann, B., Nacke, B.: Functional materials on the base of lanthanum chromite. In: Proceedings of the Third International Forum on Strategic Technologies IFOST 2008. Novosibirsk-Tomsk, 2008.

[7] Andrianov, M.A., Balkevich, V.L., Sotnikov, V.E.: Use of lanthanum chromite for making electric heaters, *Refract. Ind. Ceram.*, **21**, 592 – 596, (1980).

[8] Meadowcroft, D.B., Meier, P.G., Warren, A.C.: Hot ceramic electrodes for open-cycle MHD power generation, *Energ. Convers.*, **12**, 145 – 147, (1972).

[9] Yokokawa, H., Sakai, N., Kawada, T., Dokiya, M.: Chemical thermodynamic considerations in sintering of $LaCrO_3$-based perovskites, *J. Electrochem. Soc.*, **138**, 1018 – 1027, (1991).

[10] Groupp, L., Anderson, H.U.: Densification of $La_{1-x}Sr_xCrO_3$, *J. Am. Ceram. Soc.*, **59**, 9 – 10, (1976).

[11] Duvigneaud, P.H., Pilate, P., Cambier, F.: Factors affecting the sintering and the electrical properties of sr-doped $LaCrO_3$, *J. Eur. Ceram. Soc.*, **14**, 359 – 367, (1994).

[12] Sakai, N., Kawada, T., Yokokawa, H., Dokiya, M., Kojima, I.: Liquid-Phase-assisted sintering of calcium-doped lanthanum chromites, *J. Am. Ceram. Soc.*, **76**, 609 – 616, (1993).

[13] Mori, M., Yamamoto, T., Ichikawa, T., Takeda, Y.: Dense sintered conditions and sintering mechanisms for alkaline earth metal (Mg, ca and Sr)-doped $LaCrO_3$ perovskites under reducing atmosphere, *Solid State Ionics*, **148**, 93 – 101, (2002).

[14] Carter, J.D., Nasrallah, M.M., Anderson, H.U.: Liquid phase behavior in nonstoichiometric calcium-doped lanthanum chromites, *J. Mater. Sci.*, **31**, 157 – 163, (1996).

[15] Simner, S.P., Hardy, J.S., Stevenson, J.W., Armstrong, T.R.: Sintering of lanthanum chromite using strontium vanadate, *Solid State Ionics*, **128**, 53 – 63, (2000).

[16] Chick, L.A., Pederson, L.R., Maupin, G.D., Bates, J.L., Thomas, L.E., Exarhos, G.J.: Glycine-nitrate combustion synthesis of oxide ceramic powders, *Mater. Lett.*, **10**, 6 – 12, (1990).

[17] Purohit, R.D., Sharma, B.P., Pillai, K.T., Tyagi, A.K.: Ultrafine ceria powders via glycine-nitrate combustion, *Mater. Res. Bull.*, **36**, 2711 – 2721, (2001).

[18] Toniolo, J.C., Lima, M.D., Takimi, A.S., Bergmann, C.P.: Synthesis of alumina powders by the glycine-nitrate combustion process, *Mater. Res. Bull.*, **40**, 561 – 571, (2005).

[19] Bošković, S.B., Djurović, D.R., Zec, S.P., Matovic, B.Z., Zinkevich, F., Aldinger, F.: Doped and Co-doped CeO_2: preparation and properties, *Ceram. Int.*, **34**, 2001 – 2006, (2008).

[20] Bošković, S.B., Matovic, B.Z., Vlajić, M.D., Kristić, V.D.: Modified glycine nitrate procedure (MGNP) for the synthesis of SOFC nanopowders, *Ceram. Int.*, **33**, 98 – 93, (2007).

[21] Liu, X., Su, W., Lu, Z.: Study on synthesis of $Pr_{1-x}Ca_xCrO_3$ and their electrical properties, *Mater. Chem. Phys.*, **82**, 327 – 330, (2003).

[22] Kikukawa, N., Takemori, M., Nagano, Y., Sugasawa, M., Kobayashi, S.: Synthesis and magnetic properties of nanostructured spinel ferrites using a glycine-nitrate process, *J. Magn. Magn. Mater.*, **284**, 206 – 214, (2004).

[23] Valefi, M., Falamaki, C., Ebadzadeh, T.: New insights of the glycine-nitrate process for the synthesis of nano-crystalline 8YSZ, *J. Am. Ceram. Soc.*, **90**, 2008 – 2014, (2007).

[24] Vijayan, L., Cheruku, R., Govinadaraj, G., Rajagopan, S.: Physical and electrical properties of combustion synthesized NASICON type $Na_3Cr_2(PO_4)_3$ crystallites: effect of glycine molar ratios, *Mater. Chem. Phys.*, **130**, 862 – 869, (2011).

[25] Zhuravlev, V.D., Vasil'ev, V.G., Vladimirova, E.V., Shevchenko, V.G., Grigorov, I.V., Bamburov, V.G., Beketov, A.R., Baranov, M.V.: Glycine-nitrate combustion synthesis of finely dispersed alumina, *Glass Phys. Chem.*, **36**, 506 – 512, (2010).

[26] Jain, S.R., Adiga, K.C., Verneker, V.R.P.: A new approach to thermochemical calculations of condensed fuel-oxidizer mixtures, *Combust. Flame*, **40**, 71 – 79, (1981).

[27] Nair, S.R., Purohit, R.D., Tyagi, A.K., Shina, P.K., Sharma, B.P.: Role of glycine-to-nitrate ratio in influencing the powder characteristics of $La(Ca)CrO_3$, *Mater. Res. Bull.*, **43**, 1573 – 1582, (2008).

[28] Shao, Z., Zhou, W., Uhu, Z.: Advanced synthesis of materials for intermediate-temperature solid oxide fuel cells, *Prog. Mater. Sci.*, **57**, 804 – 874, (2012).

[29] Chick, L.A., Liu, J., Stevenson, J.W., Armstrong, T.R., McCready, D.E., Maupin, G.D., Coffey, G.W., Coyle, C.A.: Phase transitions and transient liquid-phase sintering in calcium-substituted lanthanum chromite, *J. Am. Ceram. Soc.*, **80**, 2109 – 2120, (1997).

[30] Ianculescu, A., Braileanu, A., Pasuk, I., Zaharescu, M.: Phase formation study of alkaline earth-doped lanthanum chromites, *J. Therm. Anal. Calorim.*, **66**, 501 – 507, (2001).

[31] Zupan, K., Pejovnik, S., Maček, J.: Synthesis of nanometer crystalline lanthanum chromite powders by the citrate-nitrate autoignition reaction, *Acta Chim. Slov.*, **48**, 137 – 145, (2001).

[32] Nair, S.R., Purohit, R.D., Sinha, P.K., Tyagi, A.K.: Sr-doped $LaCoO_3$ through acetate-nitrate combustion: Effect of extra oxidant NH_4NO_3, *J. Alloy. and Compd.*, **477**, 644 – 647, (2009).

[33] Biamino, S., Badini, C.: Combustion synthesis of lanthanum chromite starting from water solutions: Investigation of process mechanism by DTA-TGA-MS, *J. Eur. Ceram. Soc.*, **24**, 3021 – 3034, (2004).

[34] Fagerlund, G.: Determination of specific surface by the BET method, *Matériaux et Construction*, **6**, 239 – 245, (1973).